Crystallization:
finding the right annealing parameters

On behalf of
Virgo Coating R&D Collaboration
Crystallization RL

Virgo Week 02 November 2020

Coating Thermal Noise power spectrum

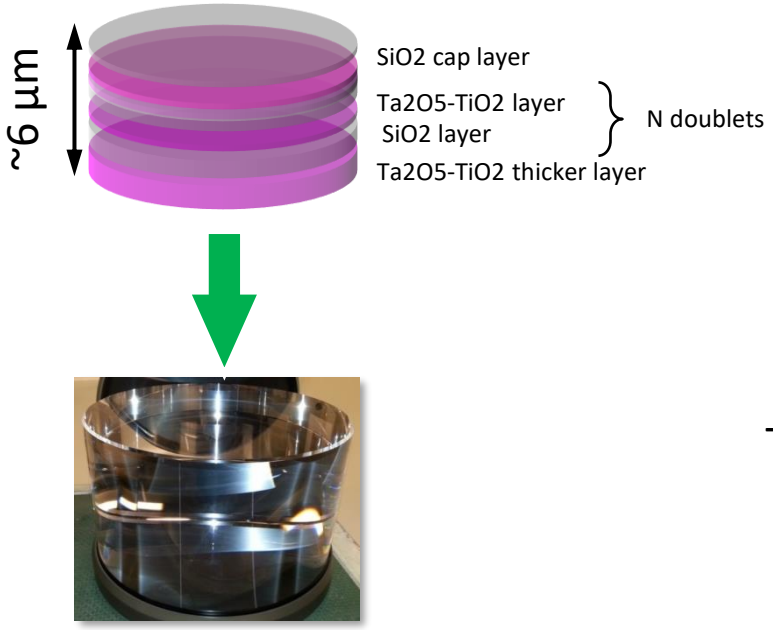

Harry et al, Class. Quantum Grav. 19 (2002)

In a Fabry-Perot geometry:

$$S_{\mathrm{CTN}} \propto T \frac{d\phi}{w^2}$$

- T: Temperature
- d: Coating thickness
- ϕ: **Mechanical Loss angle**
- w: Beam Waist

Lossy materials are noisy!

Annealing process to reduce mechanical losses

Effect of crystallization on losses still not well understood and controlled

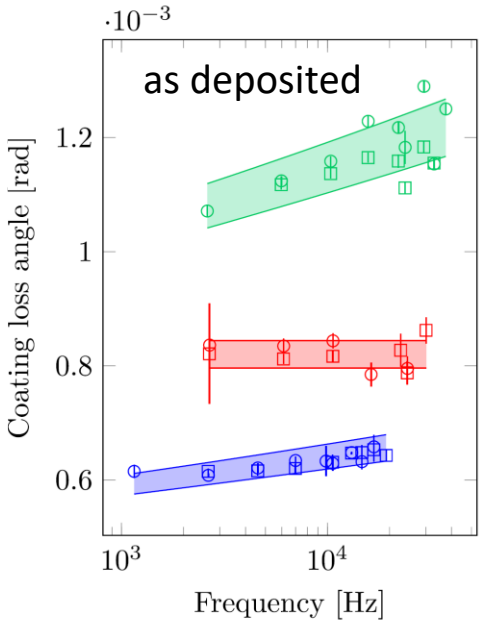

Ta_2O_5

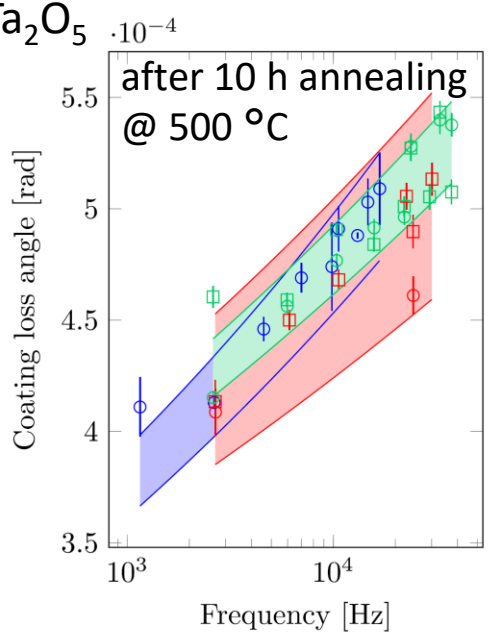

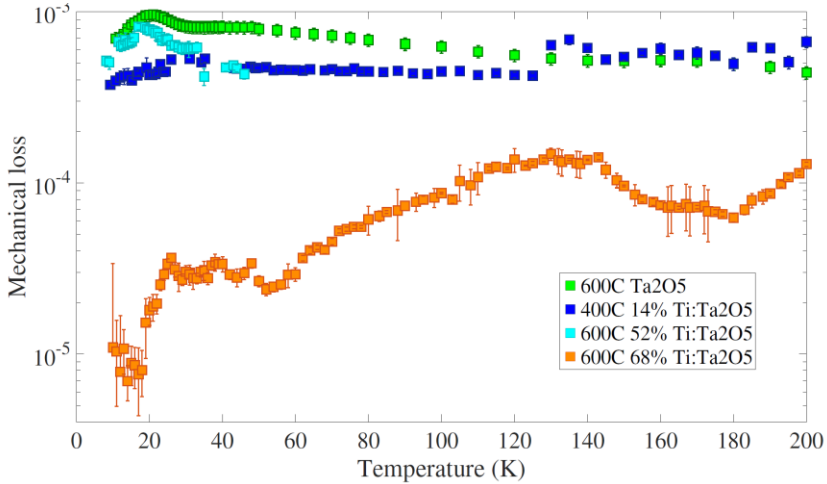

- M Granata et al 2020 Class. Quantum Grav. 37 095004
- R. Robie, Ph D Thesis, University of Glasgow, 2018

"….while displaying low mechanical loss, this coating has visual evidence of crystallization"

Post-deposition annealing process brings the structure of material coatings down to a stable optimal configuration for lowest loss. Often, but not always, crystallization can be detrimental.

The Crystallization strategy

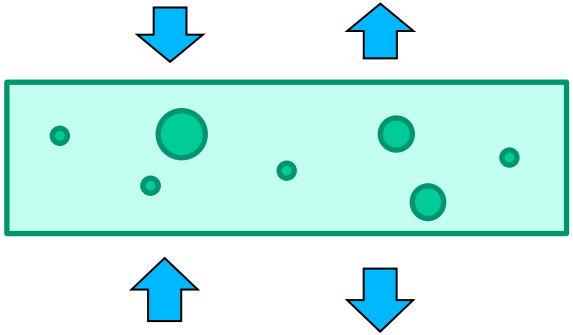

Improve the mechanical properties by favoring the controlled formation of nanocrystals inside the amorphous matrix!

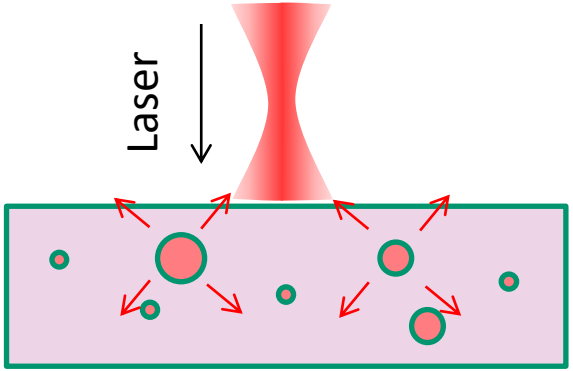

However: avoid scattering form the nanocrystals

Required:

- Precise control of the crystallization process
- Optical and mechanical characterization
- Theoretical modelling

Crystallization from the Amorphous state

Crystallization kinetics depends on:

- Nucleation rate
- Growth rate

$$N(T) = f_0(T)\exp(-g^*/RT)$$

$$g^*_{3D} = 16\pi\gamma^3/3\Delta G^2$$

$$\Delta T = T_m - T$$

$$\Delta G \approx \Delta S_m \cdot \Delta T = \Delta H_m \cdot \Delta T/T_m$$

$$g^*_{3D}(T) \sim 1/\Delta T^2.$$

Non monotonic Nucl rate

Critical 3D nucleus

$$r^*_{3D}(T) \sim 1/\Delta T$$

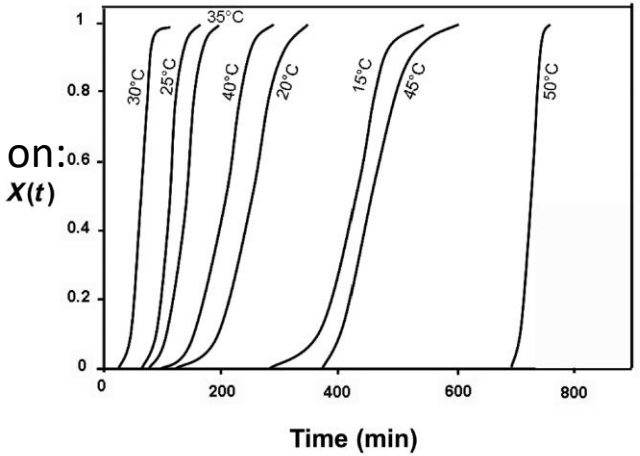

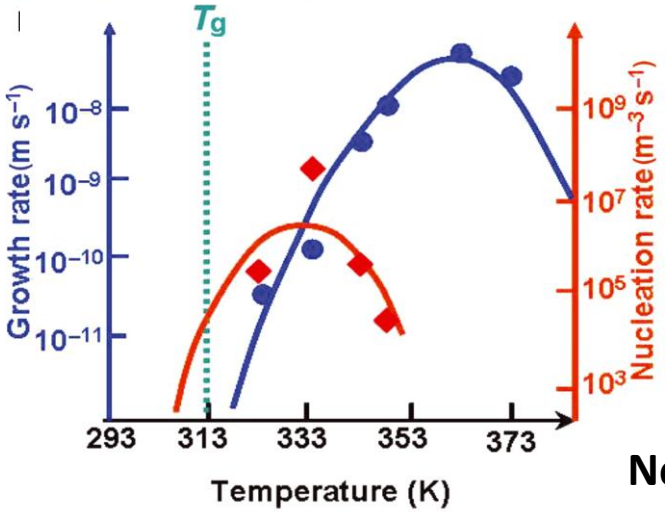

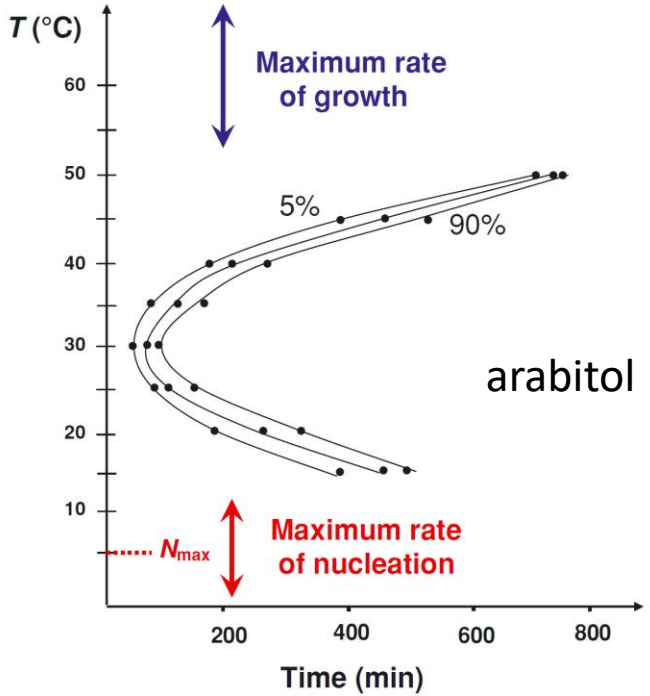

arabitol

- M Descamps et al 2014 J. Pharm. Sci. 103 2615

$$V(T) \propto V_0(T) \cdot \Omega \cdot [1 - \exp(-\Delta G/RT)]$$

$$V_0(T) \propto \exp(-\Delta G_a/RT)]$$

Non monotonic growth rate

Crystallization Theory

JMAK equation

$$x = 1 - \exp[-(kt)^n]$$

Fraction of crystallized material

Time

Rate constant

Avrami parameter

Assumptions:

- Random and homogeneous nucleation;
- Constant and isotropic growth rate;
- Growth rate does not depend upon the fraction of crystallized volume.

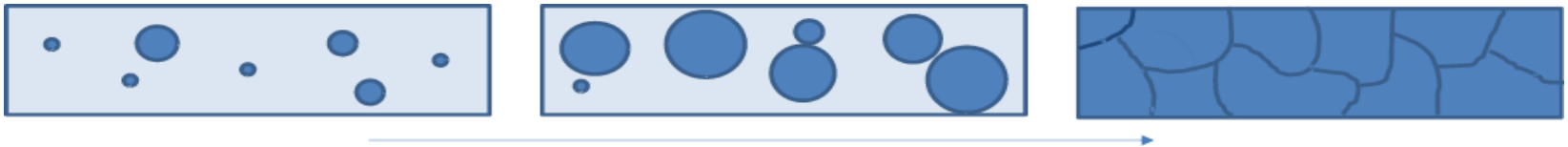

Avrami parameter values:

- Constant nucleation and interface controlled growth → n=4
- Constant nucleation and diffusion controlled growth → n=5/2
- Saturated nucleation and interface controlled growth → n=3

Rate constant follows an Arrhenius-like law:

$$k(T) = A\exp[\frac{-E_a}{k_B T}]$$

Samples and Experiment

Samples:
500nm-thick films of a-Ta_2O_5 deposited on Si substrates by Ion Beam Sputtering @ LMA (France)

Experiment:
Samples heated at fixed temperatures and monitored with Grazing Incidence X-Ray Diffraction @ INFN and Unversity of Padova (Italy)

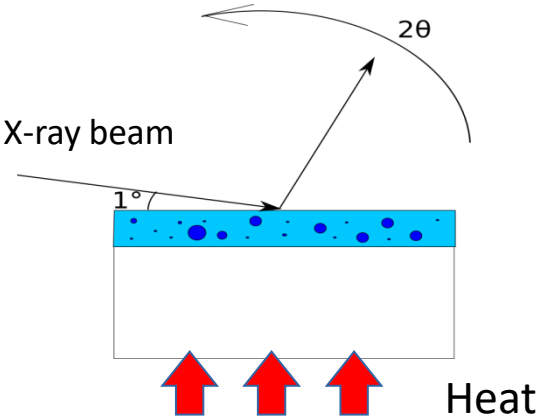

Goal:
Studying the crystallization kinetics of amorphous Ta_2O_5 thin films.

Structure assignment

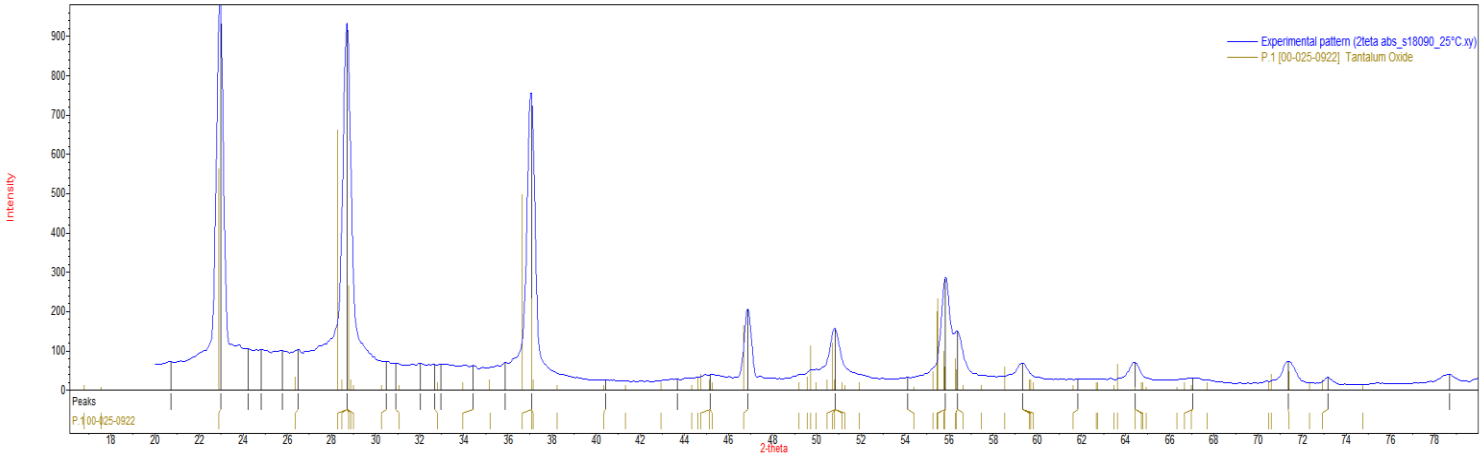

Diffraction spectrum of a crystallized sample

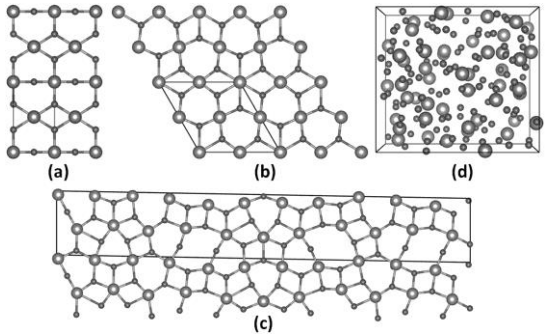

The Ta – O system crystallizes in many different polymorphs.
The assignment of the diffraction spectrum is still under discussion (probably orthorombic β-Ta_2O_5)

J. Lee; et al.; *Appl. Phys. Lett.* **105,** 202108 (2014)

Ta_2O_5 Thin Films Crystallization

Measurements focused on the (001) peak of orthorombic Ta_2O_5

Peak height proportional to crystallized volume.

Peak FWHM inversely proportional to crystallite size. (Scherrer's formula)

$$D = k\frac{\lambda}{\Delta \cos\theta}$$

- D = crystallite size
- λ = wavelength of the incident beam
- Δ = peak FWHM
- 2θ = peak position in the spectrum

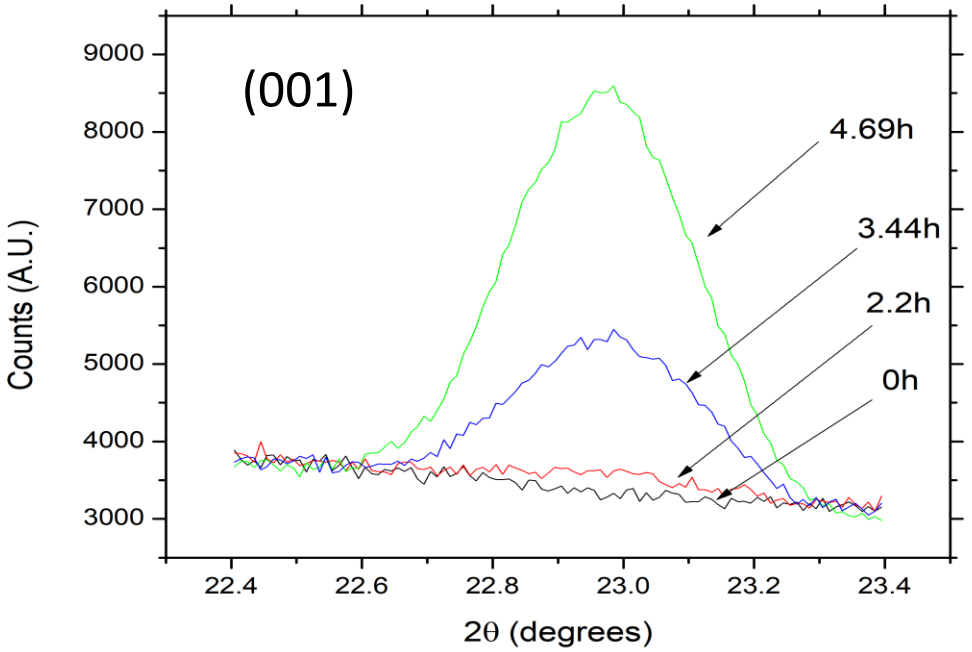

Ta_2O_5 Thin Films Crystallization

JMAK equation

$$x = 1 - \exp[-(kt)^n]$$

- x → Fraction of the crystallized volume.
- $n = D + 1$ → information about the dimensionality D of the growth.
- k →crystallization rate

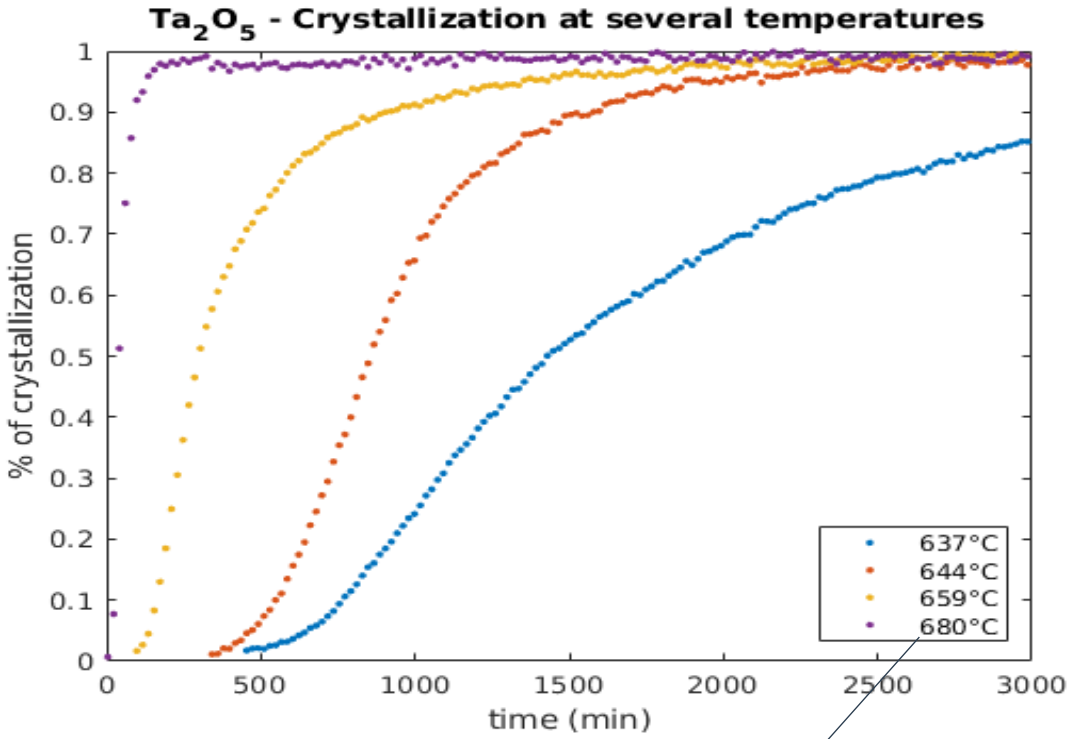

Temperatures corrected for substrate thermal conductivity

Avrami Plots

Linearized JMAK equation:

$$\ln[1 - \ln x] = n \ln t + n \ln k$$

From the fit of the first part of the curves:

$$n = 4.11 \pm 0.05$$

Strong indication of a constant nucleation rate and a 3D growth

Highly homogeneous films

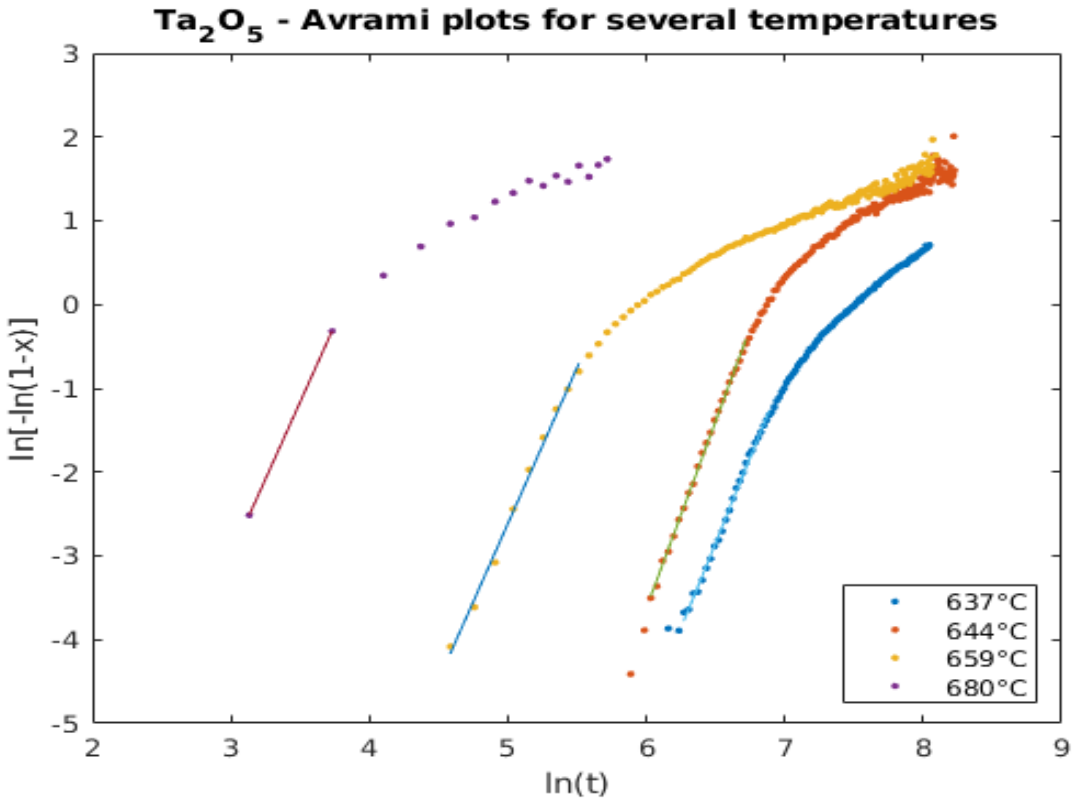

Activation Energy

Arrhenius' law:

$$k(T) = A\exp[\frac{-E_a}{k_B T}]$$

$$\ln(k) = \ln(A) - \frac{E_a}{k_B T}$$

$$E_a = 290 \pm 20\, kJ/mol$$

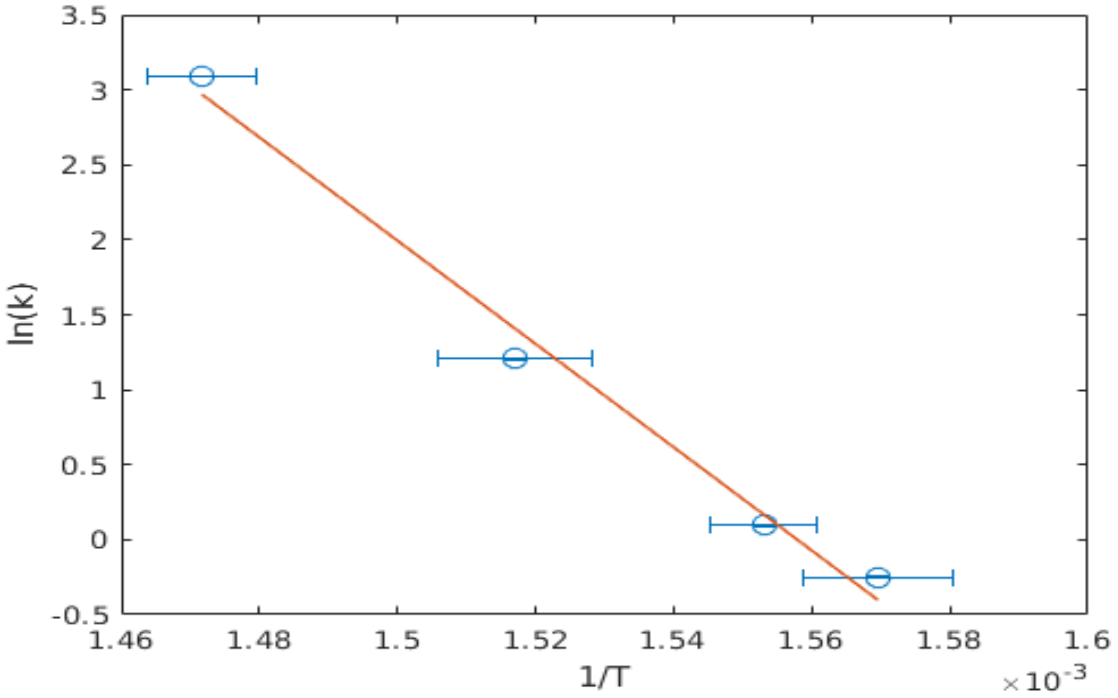

Average Cristallite Size

Average crystallite size estimated with Scherrer's formula after correcting for instrumental broadening:

$$D = \frac{\lambda k}{\Delta \cos(\theta)}$$

- Crystallites start to be detected when they are already around 17 - 18 nm.
- The final average crystallite size appears to depend on the annealing temperature, which is reasonable from thermodynamic arguments.

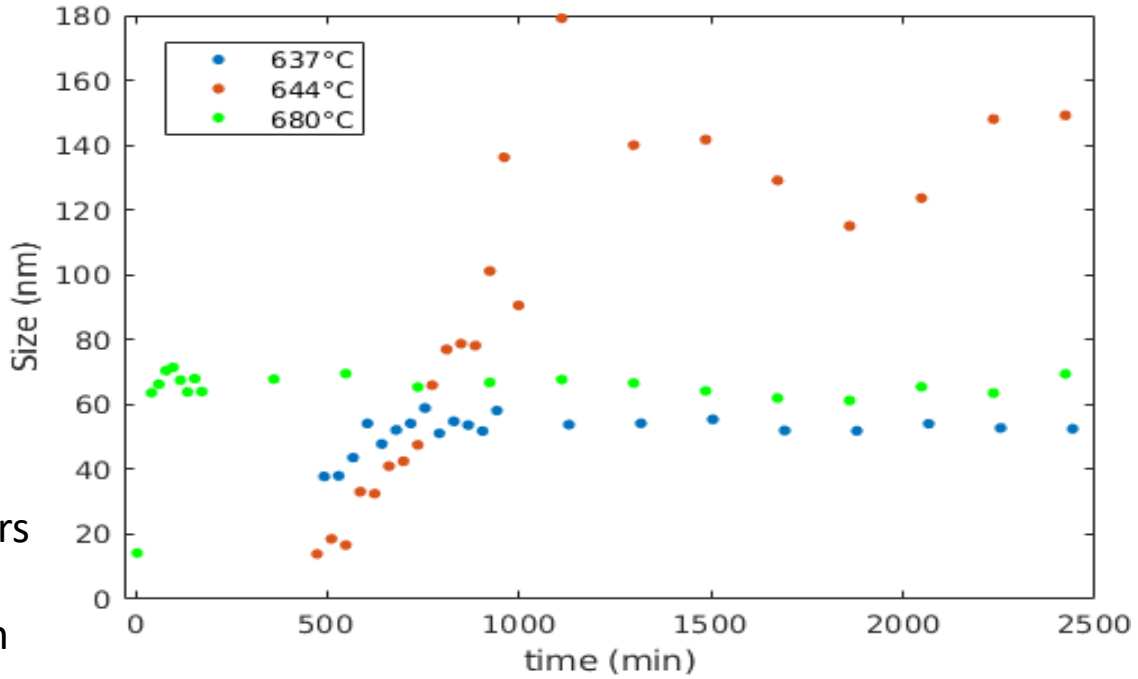

Different behavior for TiO2

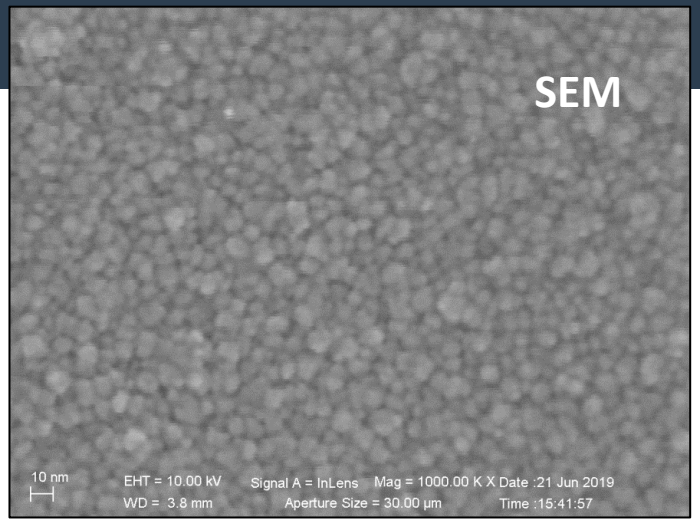

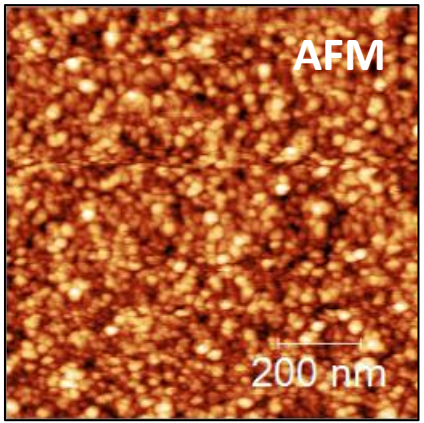

On the contrary of Tantala, those samples present an evident grain structure already after the deposition.

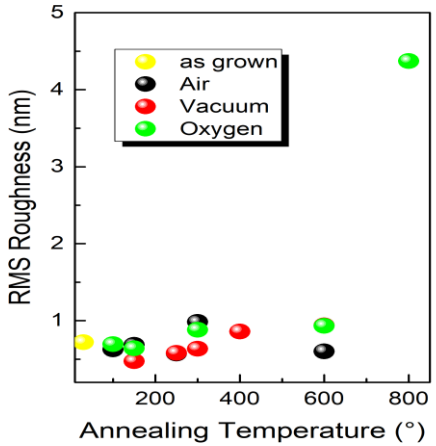

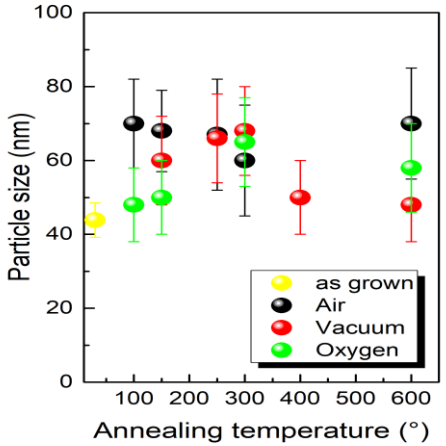

Those «grains» remain essentially unchanged up to 600°C, independently on the annealing atmosphere.

TiO_2 Crystallization kinetics @ 200°C

XRD data taken around the TiO_2 (101) peak at 25.3°

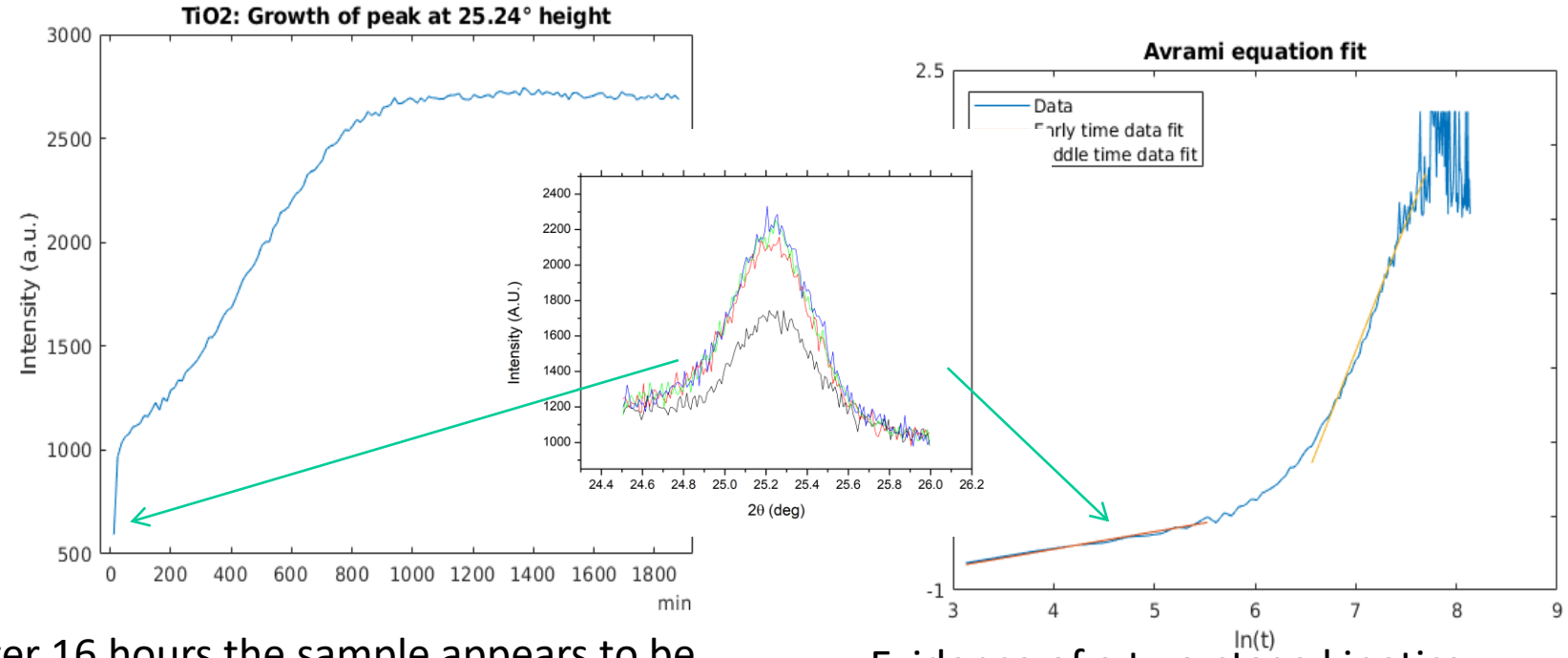

After 16 hours the sample appears to be fully crystallized

Evidence of a two-stage kinetics:
n<3 => low dimensinality

Ex-situ XRD on TiO2 samples after annealing

Data from UniSannio/Salerno

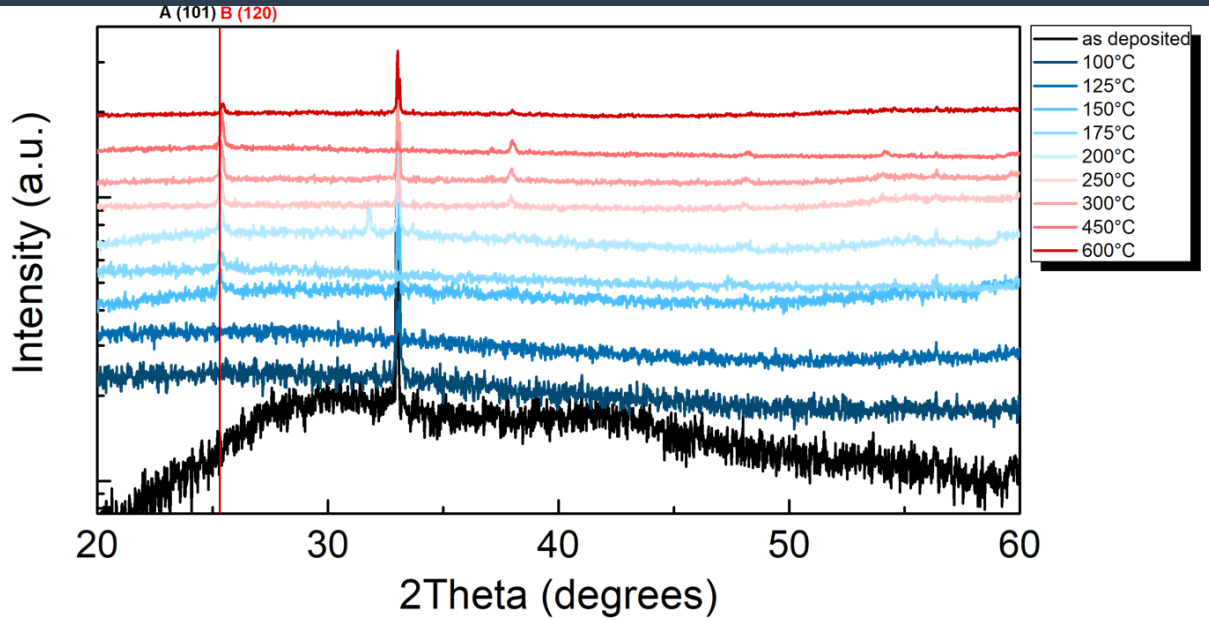

- Higher temperature annealing produce a stronger peak (also confirmed by Raman).
- However, in-situ XRD showed that an equilibrium condition was reached after 16 hours (and less for higher temp).

The equilibrium $\frac{V_C}{V_{TOT}}$ depends on the temperature.

A tentative explanation: crystallization at the grain boundaries

FACTS

- The as-dep- TiO2 film is grain-structured with a typical grain size around 60nm.
- The growth kinetics occurs in two stages, the first part with a dimension index $n < 3$
- The equilibrium $\frac{V_C}{V_{TOT}}$ depends on the temperature.

TENTATIVE EXPLANATION (suggested by F. Bobba)

- Crystallization occurs at the interface between the grains (energetically favorable?)
- The ratio $(V_C/V_{TOT})_{eq}$ is determined by several energetic contributions (surface tension, strain, crystal internal energy etc.) and is very likely to be T dependent.

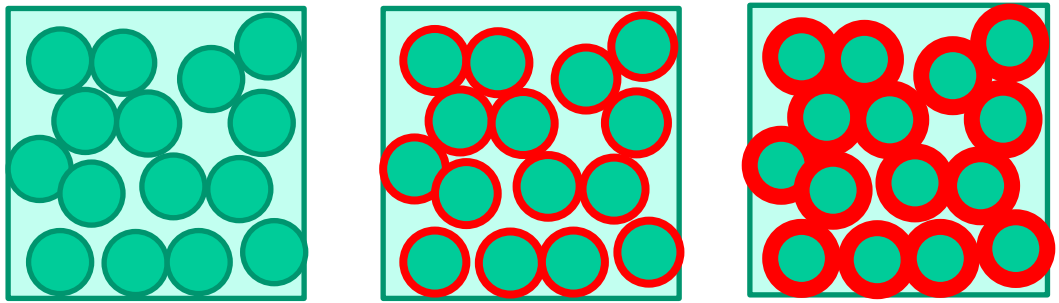

As dep | Annealed @ 200°C | Annealed @400°C

More on

Crystallization of Titania coatings

From Sannio/Sa

AFM study of TiO_2 vs thickness – IN AIR

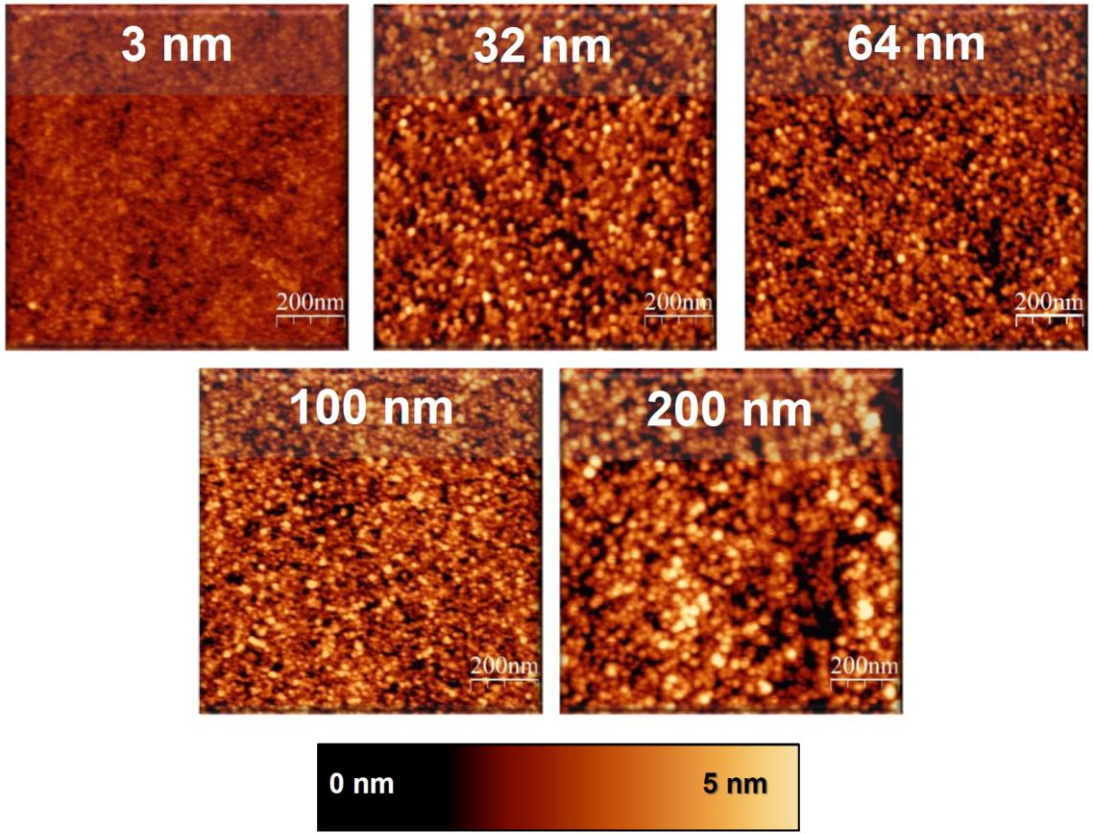

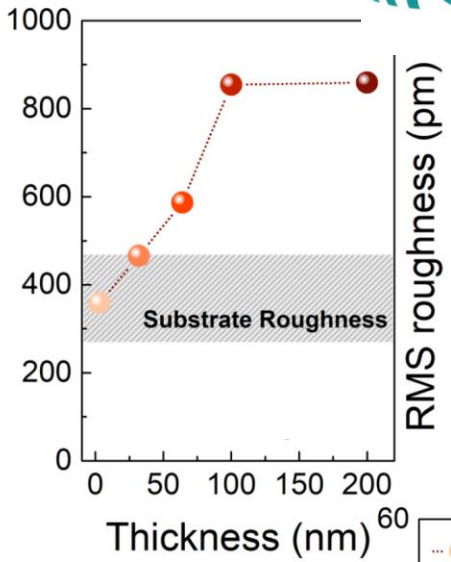

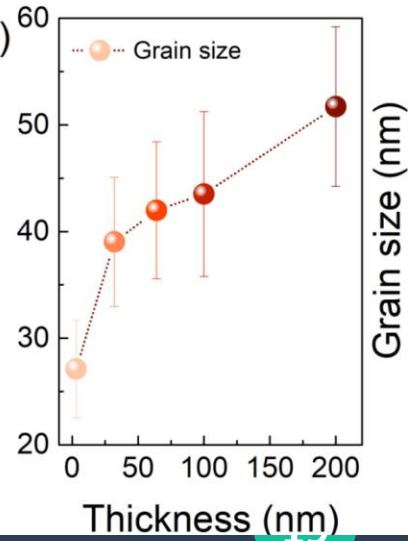

Reducing TiO_2 thickness causes the improvement of both RMS roughness and granularity.
A non-negligible overestimate of the particle size, by AFM, is more and more pronounced as their size becomes comparable to the AFM-probe's curvature radius.

Crystallization of TiO2 vs thickness – Raman Spectroscopy

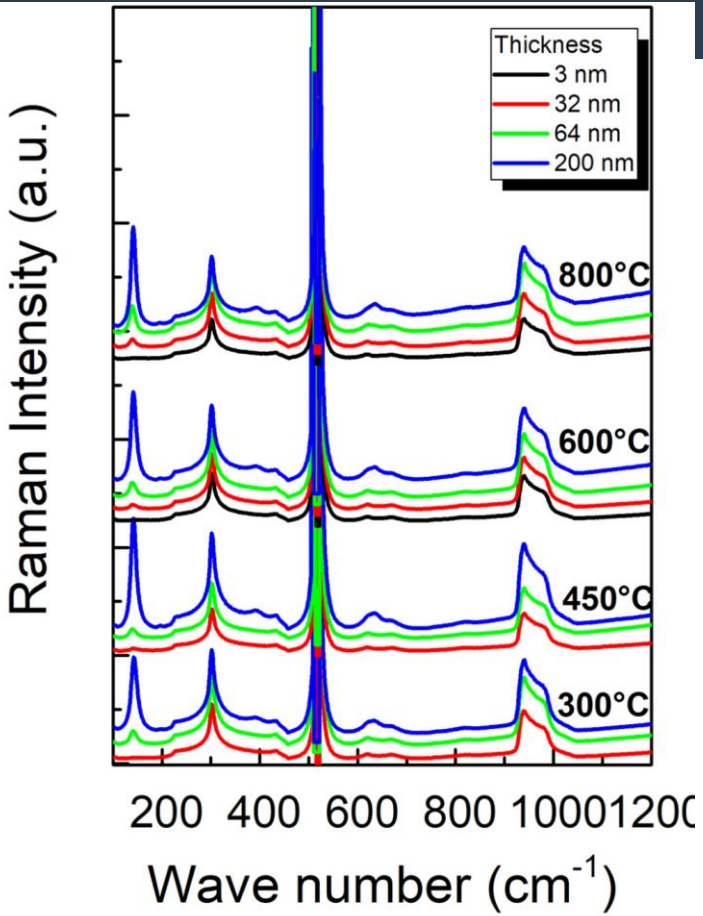

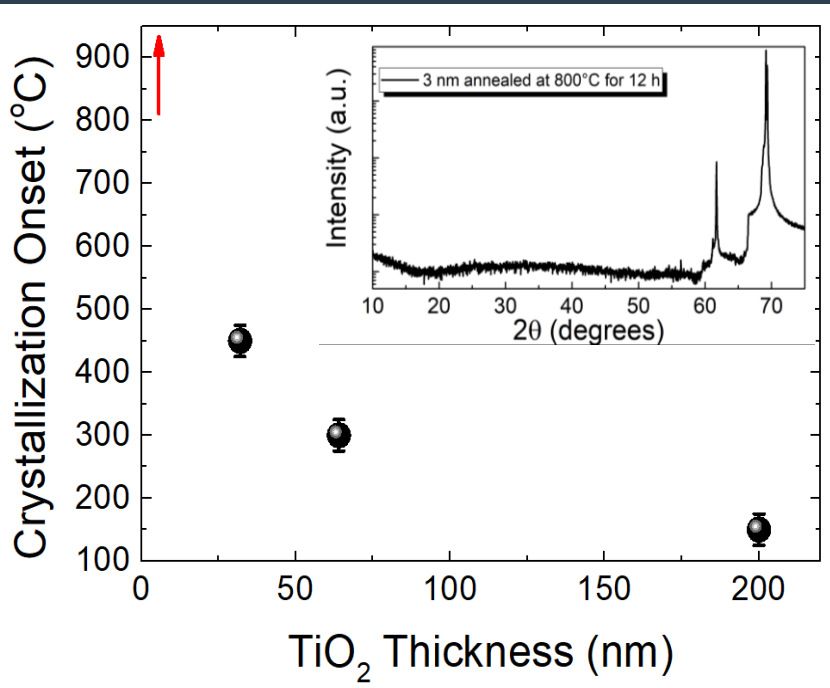

- The crystallization onset T of 3nm-TiO_2 is higher than 800°C , as confirmed by XRD (in the inset – no crystalline peaks are present).

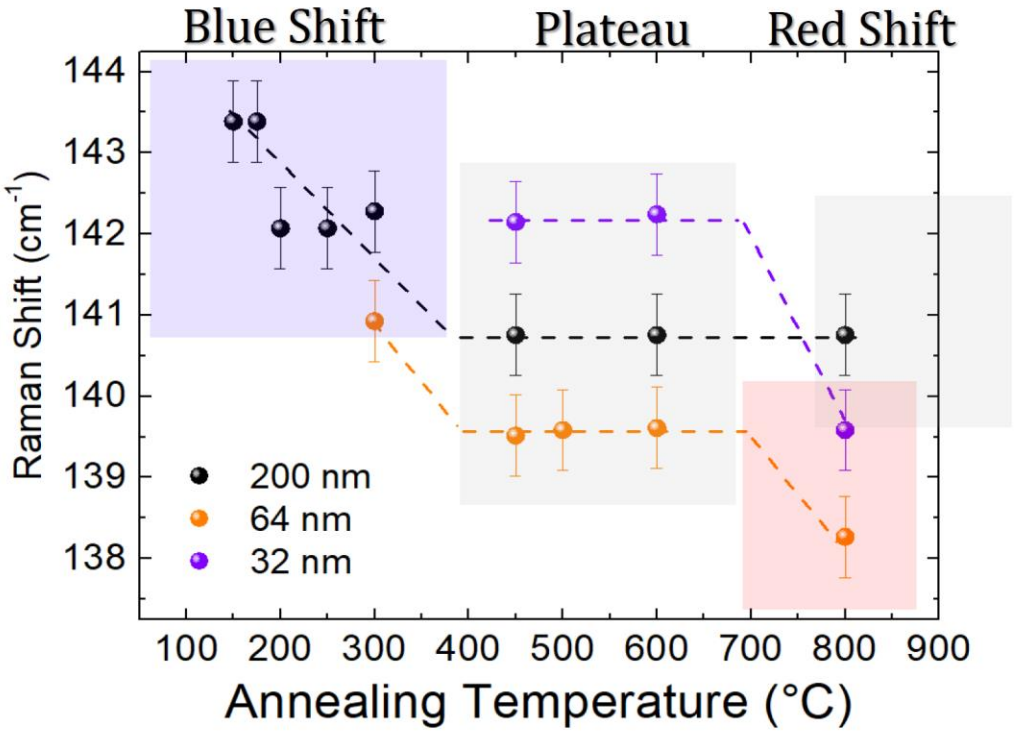

- The blueshift is possibly due to phonon confinement.
- The redshift shown by the 64nm and 32nm samples, between 600°C and 800°C, may be related to the presence of stress/strain due to the formation of "linear" structures. Those structures, which are never present in the 200nm, may be the manifestation on the surface of the top-most edge of plates cutting the film across the transversal direction.

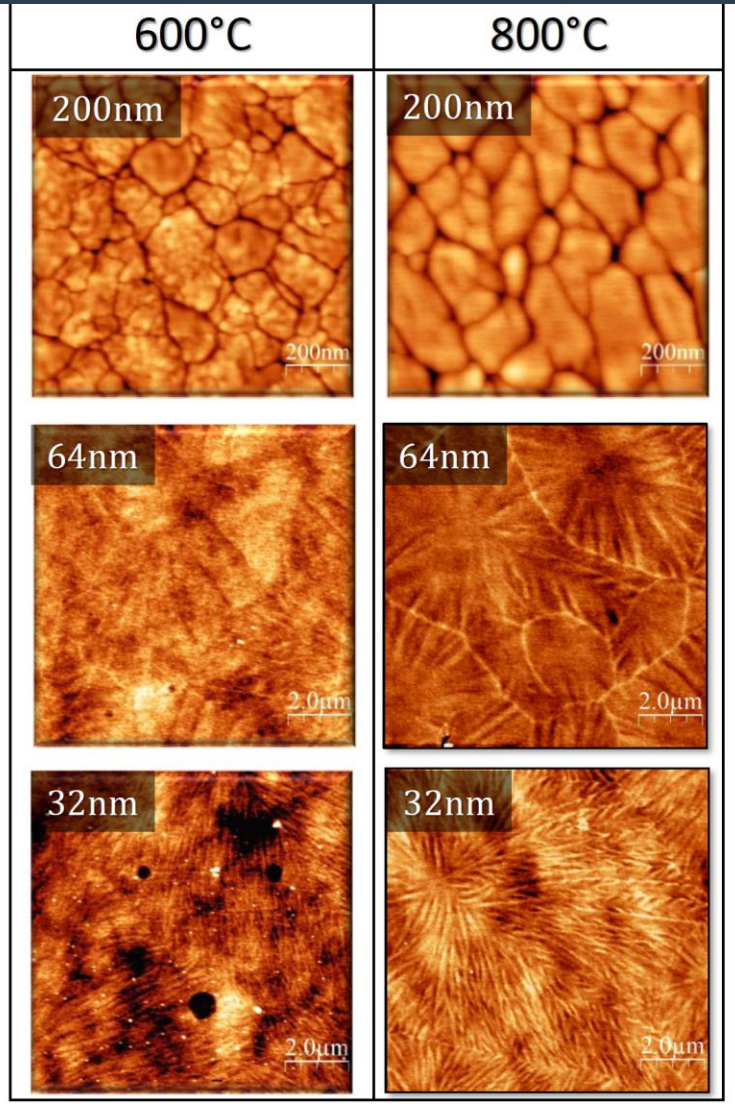

Important update SiO2-TiO2

Crystallization results on nanolayers - Summary

Sample	Nominal Thickness (nm)		Corrected Thickness (nm)		Annealing temperature (°C) in air for 12 h Crystallization Yes/No											
	TiO_2	SiO_2	TiO_2	SiO_2	AD	100	150	250	300	350	400	450	500	550	600	800
Single TiO_2	200(x1)	-			No	No	Yes									
2-layers	64(x1)	64(x1)	66.0±2.0	64.4±1.0	No	No	No	No	Yes	Yes						
4-layers	32(x2)	32(x2)	32.9±0.2	32.5±1.0	No	No	No	No	Yes	Yes						
11-layers	17.2(x5)	6.9(x6)	18.0±0.2	7.3±0.1	No	-	-	-	Yes	Yes						
19-layers	9.5(x9)	4.2(x10)	10.1±0.1	4.6±0.1	No	-	-	-	-	Yes						
45-layers	3.9(x22)	1.8(x23)	4.5±0.1	2.2±0.1	No	No	No	No	No	No	Yes					
76-layers	2.0(x38)	1.3(x38)	3.05±0.06	0.75±0.11	No	No	No	No	No	No	No	No	No	No	No	No
85-layers	2.1(x42)	0.9(x43)	3.2±0.1	1.3±0.1	No	No	No	No	No	No	No	No	No	No	No	No

TiO_2 top surface

SiO_2 top surface

First Optical Tests on Tantala

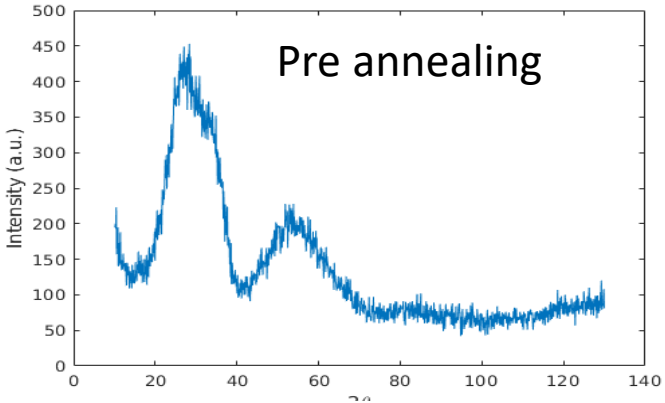

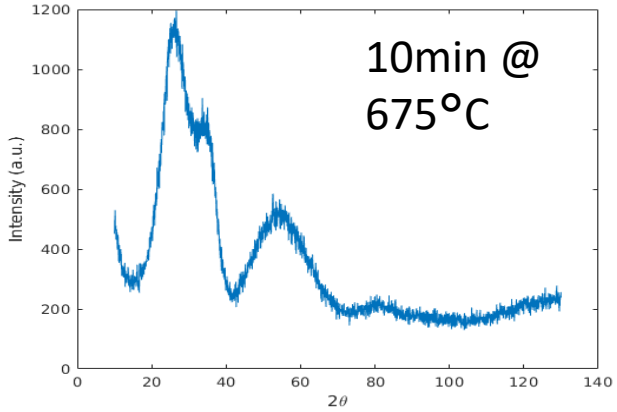

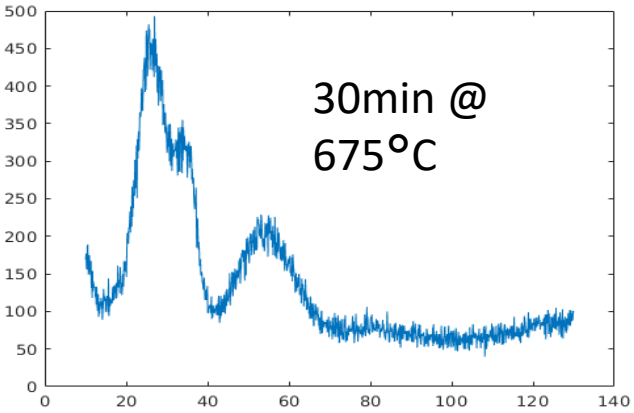

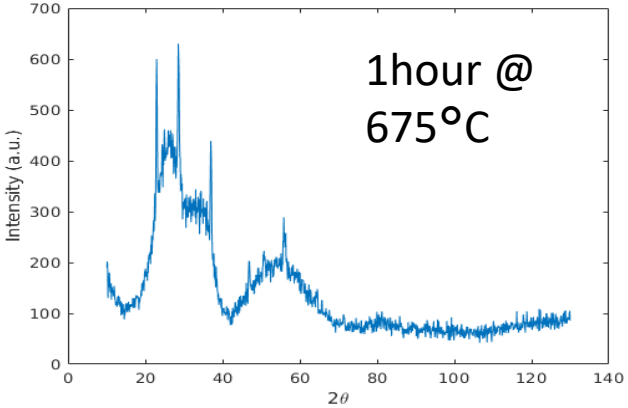

A set of samples with varying crystallization degrees have been prepared and are now undergoing structural/optical characterizations

First Test: light scattering @ LMA in progress

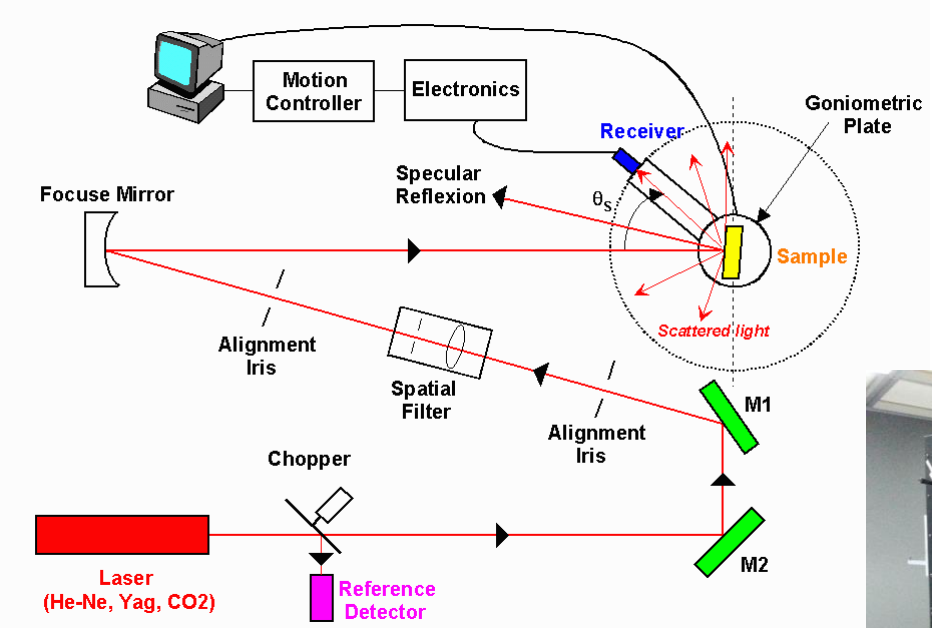

A set of samples with varying crystallization degrees are under test for light scattering

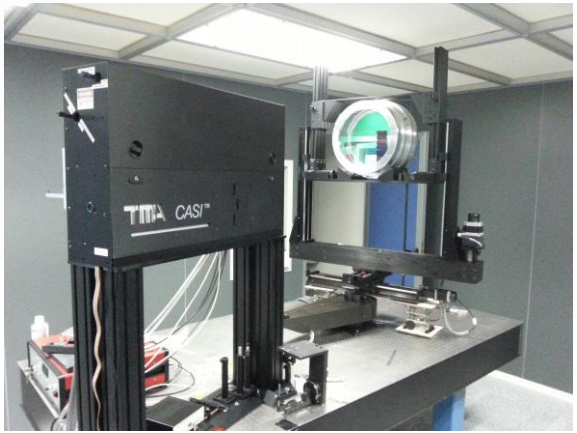

In progress

Problems

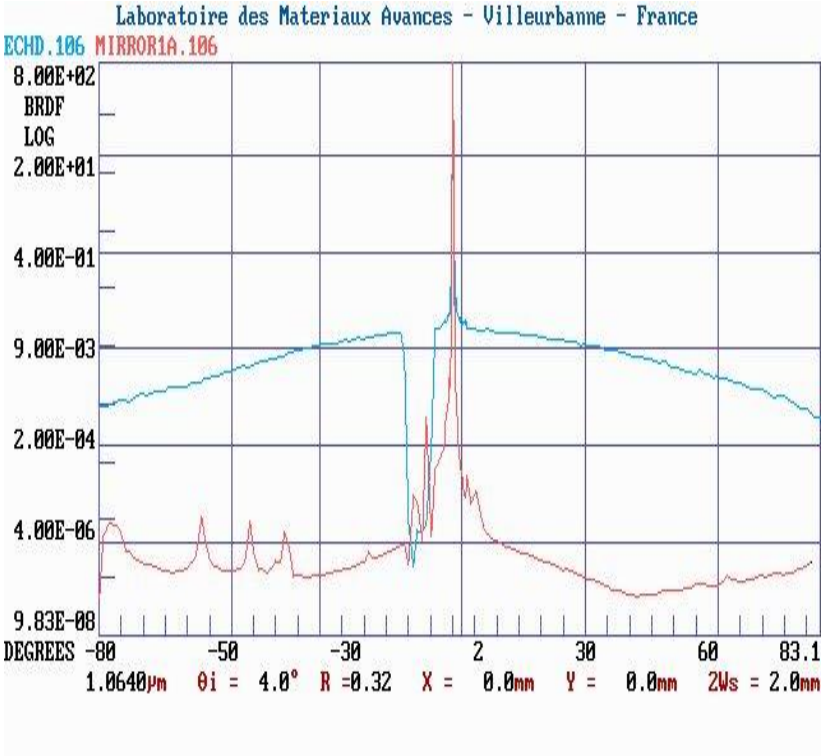

BDRF for sample treated 10 mins

However the BDRF shows a very strong scattering for all the three samples, apparently not correlated with the treatment duration.

Investigation is going on:
In order to understand the origin of such a huge scattering, samples have been further analysed.

Problems

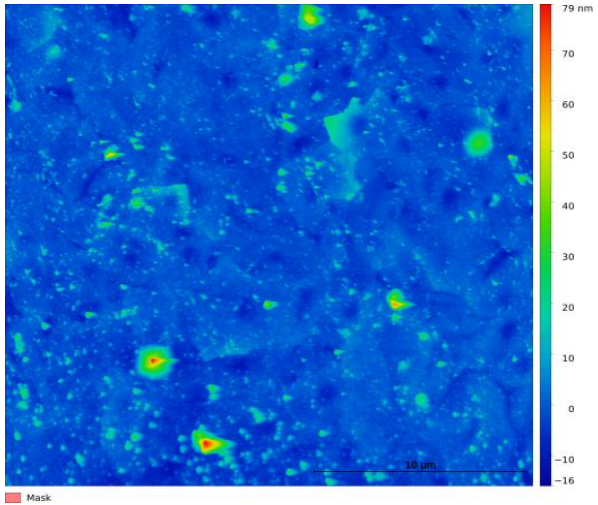

Untreated

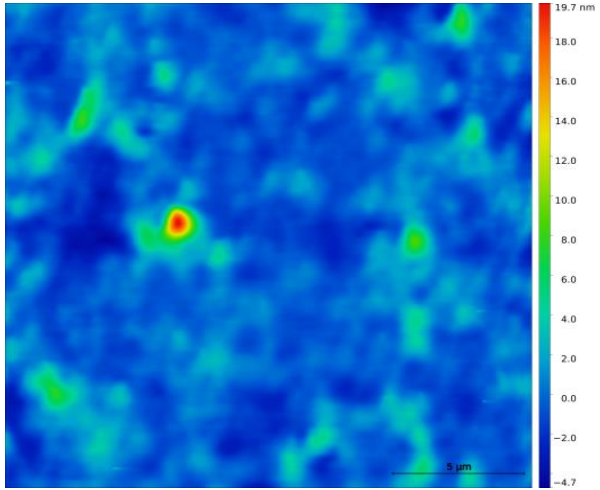

Sample treated 10 min @685°C

AFM analysis =>
very high surface roughness.

Both on thermally treated samples and on our untreated reference sample
=> thermal treatment is not the ultimate responsible for the surface deterioration.

Maybe it can be attributed to insufficient care in handling and storing the samples.
Now: cleaning the samples and checking for surface contamination.

Conclusions (1)

- Crystallization kinetic of 500nm-thick films of a-Ta_2O_5 produced by IBS has been investigated;
- The crystallization is characterized by a homogeneous nucleation and a 3D growth in the first stage;
- The activation energy of the process has been estimated: **E_a = 290 ± 20 kJ/mol;**
- the as-formed crystallites have a size of the order of 20 nm and grow further to fnal size which seems to depend on the annealing temperature;
- Degree of crystallization and size of nanocrystals can be tuned at suitable annealing temperatures and times
- Samples with a low degree of crystallization have been prepared and are going to be optically and mechanically tested

Scattering by nanocrystals in the mirrors of future gravitational wave detectors

MARGHERITA SIMONI, ELISABETTA CESARINI

EXCERP FROM VIR-0853A-20 ON TDS

Controlled crystallization

❖ We are interested in the crystallization process because the annealing process used to reduce the mechanical losses crystallizes the amorphous film. For those materials that crystallize at lower temperatures (eg. 600°C) the scattering of light on the nanocrystals could cause a non negligible optical loss.

❖ We can model the transformation process from the amorphous phase to the crystalline phase, which occurs when the material is heated, studying the cinematic of crystallization. The transformation happens in two steps: nucleation and growth– [ref. *Low noise mirror coatings for next generation gravitational-wave detectors,* Giacomo Lorenzin.]

❖ We want to model the attenuation due to scattering, and define a limit in terms of size and density of the nanocrystals, to keep the optical losses within the requirements of future gravitational waves detectors.

❖ Materials: **Tantalum pentoxide, or tantala** (Ta_2O_5)**, Titanium dioxide, or titania (TiO_2) Zirconium dioxide, or zirconia (ZrO_2)**

Scattering by nanoparticles

We want to define the optical losses due to scattering, in terms of the density of the number of nanocrystals and their sizes

The losses are given by the number of scattered photons compared to the incident ones. Or from an energy point of view:

$$L_{scatt} = \frac{N_{scatt}}{N_{TOT}} = \frac{I \cdot S_{scatt}}{I \cdot S_{TOT}} = \frac{S_{scatt}}{S_{TOT}} = \frac{\sigma \cdot n}{\pi w^2} = \frac{\sigma \cdot \rho_S \pi w^2}{\pi w^2} = \sigma \cdot \rho_S$$

S_{scatt}= scattering surface
S_{TOT}= surface where the scattering occours
w=radius of S_{TOT}
σ=scattering cross section
n= number of nanoparticles
ρ_S=superficial density
t=thickness of the film

But this formula is only useful if we know the surface density. From the experimental measurements a volumetric density can be extracted, the relation $\sigma \cdot \rho_V$ will therefore give a linear attenuation coefficient, whose reciprocal is the depth of penetration:

$$\mu_{att} = \lambda^{-1} = \rho_V \sigma_{scatt}$$

The actual attenuation can be found using the formula for the intensity of the transmitted wave $I_T(t) = I_I \, e^{-\frac{t}{\lambda}}$, used in the Lambert-Beer formula:

$$L_{scatt} = \frac{I_I - I_T}{I_I} = 1 - \frac{I_T}{I_I} = 1 - e^{-\frac{t}{\lambda}} = 1 - e^{-t\rho_V \sigma_{scatt}}$$

Where I_I is the intensity of the impinging wave, and σ_{scatt} is the scattering cross section

Mie's theory

The parameter to be determined is the **scattering cross section**, which is due to diffusers that are smaller than the wavelength

Scattering of a plane electromagnetic wave that interacts with bonded particles is describe by:

- **Rayleigh's scattering** if $d<<\lambda$
- **Mie's scattering** if $d\approx\lambda$

Not being able to make a priori assumptions about the particle size, we used the more complex treatment of the diffusion phenomenon provided by Mie-Lorenz

The formula that Mie finds for the scattering cross section is:

$$\sigma_{scatt} = \frac{2\pi}{k^2}\sum_{n=1}^{\infty}(2n+1)(|a_n|^2 + |b_n|^2)$$

Where the coefficients are given by:

$$a_n = \frac{m\psi_n(mx)\psi'_n(x) - m\psi_n(x)\psi'_n(mx)}{m\psi_n(mx)\xi'_n(x) - \xi_n(x)\psi'_n(mx)}$$

$$b_n = \frac{\psi_n(mx)\psi'_n(x) - m\psi_n(x)\psi'_n(mx)}{\psi_n(mx)\xi'_n(x) - m\xi_n(x)\psi'_n(mx)}$$

With $m = \frac{k_1}{k}$, where k_1 and k are respectively the refractive index of the particle and of the medium, and ψ e ξ are the Riccati-Bessel functions.

Mie's scattering simulations

MatScat is a MATLAB package that computes the scattering of light by a sphere, based on Mie's theory. The **SCATMIE function** of the package was used to estimate the total scattering cross section.

The input data are the **refractive indices** of the amorphous medium and of the crystallite, the **particle radius** and the **wavelength** of the laser.

Making this simulation we made several assumptions:

- When we talk about volumetric density we are assuming that the crystals do not cover each other, and each one is completely invested by the photons of the beam
- Nanocrystals are formed separately
- We also approximate the nanocrystals to a spherical shape

ref: *Jan Schäfer (2020). MatScat (https://www.mathworks.com/matlabcentral/fileexchange/36831-matscat), MATLAB Central File Exchange. Retrieved October 15, 2020.*

Experimental data

Average size of the tantala crystals plotted as a function of the annealing time, for different temperatures, taken near the crystallization temperature

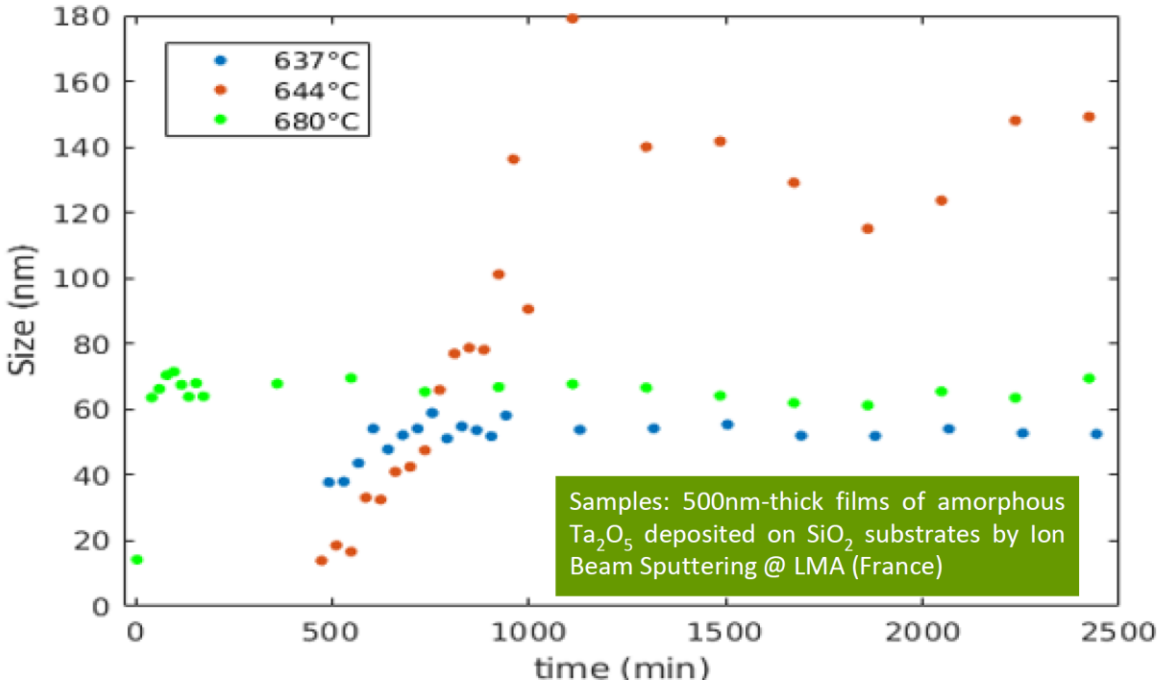

Radii of the nanocrystal

Starting from these experimental data we have chosen to vary the radii of the nanodiffusers in the simulations from 10 to 150 nm

ref. Capaccioli S. et al. G2001690-v1
https://dcc.ligo.org/LIGO-G2001690

Average crystallite size estimated with Scherrer's formula from XRD at grazing angle (Padova)

Data

Ta_2O_5 amorphous	2.05	A. Amato et al., J. Phys. Mater. 2 035004 (2019)	https://doi.org/10.1088/2515-7639/ab206e
Ta_2O_5 cristalline	2.1297	Bright et al. 2013: Nanocrystalline film n,k 0.5-1000 µm	https://refractiveindex.info/

ZrO_2 amorphous	2.10	R. Flaminio et al., Class. Quant. Grav. 27 084030 (2010)	https://doi.org/10.1088/0264-9381/27/8/084030
ZrO_2 cristalline	2.1224	Wood and nassau 1982: Cubic zirconia stabilized with yttria; n 0.361-5.14 µm	https://refractiveindex.info/

TiO_2 amorphus	2.32	M. Magnozzi et al., Opt. Mater. 75 94 (2018)	https://doi.org/10.1016/j.optmat.2017.09.043
TiO_2 Cristalline	2.175	D. Yang et al., Materials Science in Semiconductor Processing, 16, 6 (2013)	https://www.sciencedirect.com/science/article/pii/S1369800113001947

Refractive indices

Courtesy: Michele Magnozzi

Data

Densities

The densities are estimated using a critical density ρ_c, that is different for every radius:

$$\rho_c = \frac{1}{\pi r^2 t}$$

r=radius of the nanoparticle
t=thickness of the film

At this density all the material is crystalized, and it is different for every radius. We take densities that are fractions of the critical density:

$$\eta = \frac{\rho_c}{N}$$

N=10, 100, 1000, 10000

Thicknesses

$t_{ITM} = 0.727\ \mu m$

$t_{ETM} = 2.109\ \mu m$

Tantala (Ta_2O_5) ITM

parametro di vista	r=10nm	r=20nm	r=30nm	r=40nm	r=50nm
η(10)	5,19297E-08	8,17871E-07	4,03306E-06	1,22863E-05	2,86131E-05
η(100)	5,19297E-09	8,17871E-08	4,03306E-07	1,22863E-06	2,86131E-06
η(1000)	5,19297E-10	8,17871E-09	4,03306E-08	1,22863E-07	2,86131E-07
η(10000)	5,19297E-11	8,17871E-10	4,03306E-09	1,22863E-08	2,86131E-08

parametro di vista	r=60nm	r=70nm	r=80nm	r=90nm	r=100nm
η(10)	5,6018E-05	9,70045E-05	0,0001532	0,000225147	0,00031232
η(100)	5,6018E-06	9,70045E-06	1,532E-05	2,25147E-05	3,1232E-05
η(1000)	5,6018E-07	9,70045E-07	1,532E-06	2,25147E-06	3,1232E-06
η(10000)	5,6018E-08	9,70045E-08	1,532E-07	2,25147E-07	3,1232E-07

parametro di vista	r=110nm	r=120nm	r=130nm	r=140nm	r=150nm
η(10)	0,000413369	0,000526551	0,000650267	0,000783573	0,000926525
η(100)	4,13369E-05	5,26551E-05	6,50267E-05	7,83573E-05	9,26525E-05
η(1000)	4,13369E-06	5,26551E-06	6,50267E-06	7,83573E-06	9,26525E-06
η(10000)	4,13369E-07	5,26551E-07	6,50267E-07	7,83573E-07	9,26525E-07

Table of linear attenuation coefficients expressed in μm^{-1}, as a function of the density of the particle number and the radius.

Optical losses as a function of radius and densities

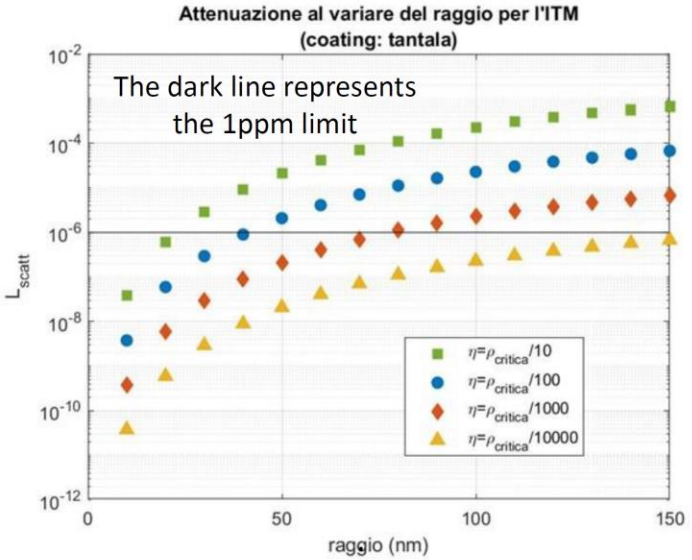

.

The current Advanced Virgo scattering losses are estimated to be at 10 ppm per mirror (J. Degallaix)

Tantala (Ta_2O_5) ETM

parametro di vista	r=10nm	r=20nm	r=30nm	r=40nm	r=50nm
η(10)	1,79008E-08	2,81931E-07	1,39025E-06	4,23525E-06	9,86333E-06
η(100)	1,79008E-09	2,81931E-08	1,39025E-07	4,23525E-07	9,86333E-07
η(1000)	1,79008E-10	2,81931E-09	1,39025E-08	4,23525E-08	9,86333E-08
η(10000)	1,79008E-11	2,81931E-10	1,39025E-09	4,23525E-09	9,86333E-09

parametro di vista	r=60nm	r=70nm	r=80nm	r=90nm	r=100nm
η(10)	1,93101E-05	3,34387E-05	5,28099E-05	7,76111E-05	0,000107661
η(100)	1,93101E-06	3,34387E-06	5,28099E-06	7,76111E-06	1,07661E-05
η(1000)	1,93101E-07	3,34387E-07	5,28099E-07	7,76111E-07	1,07661E-06
η(10000)	1,93101E-08	3,34387E-08	5,28099E-08	7,76111E-08	1,07661E-07

parametro di vista	r=110nm	r=120nm	r=130nm	r=140nm	r=150nm
η(10)	0,000142494	0,000181509	0,000224156	0,000270108	0,000319385
η(100)	1,42494E-05	1,81509E-05	2,24156E-05	2,70108E-05	3,19385E-05
η(1000)	1,42494E-06	1,81509E-06	2,24156E-06	2,70108E-06	3,19385E-06
η(10000)	1,42494E-07	1,81509E-07	2,24156E-07	2,70108E-07	3,19385E-07

Table of linear attenuation coefficients expressed in μm^{-1}, as a function of the density of the particle number and the radius.

Optical losses as a function of radius and densities

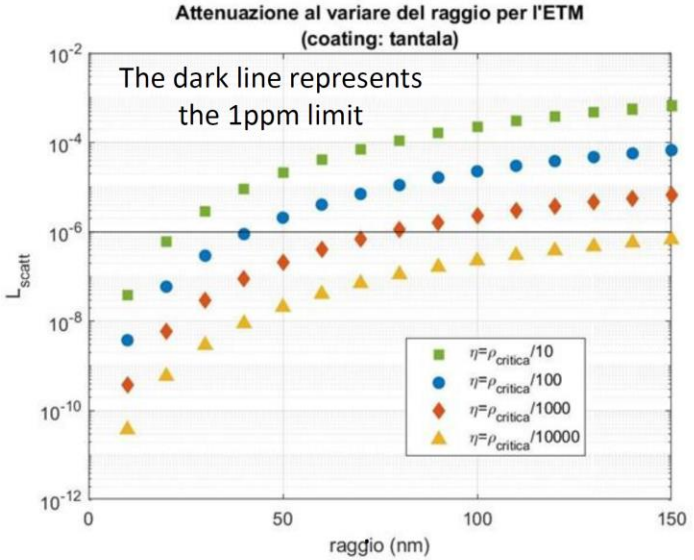

The current Advanced Virgo scattering losses are estimated to be at 10 ppm per mirror (J. Degallaix)

Titania (TiO_2) ITM

parametro di vista	r=10nm	r=20nm	r=30nm	r=40nm	r=50nm
η(10)	2,26634E-07	3,5328E-06	1,71345E-05	5,10646E-05	0,000115847
η(100)	2,26634E-08	3,5328E-07	1,71345E-06	5,10646E-06	1,15847E-05
η(1000)	2,26634E-09	3,5328E-08	1,71345E-07	5,10646E-07	1,15847E-06
η(10000)	2,26634E-10	3,5328E-09	1,71345E-08	5,10646E-08	1,15847E-07

parametro di vista	r=60nm	r=70nm	r=80nm	r=90nm	r=100nm
η(10)	0,000220306	0,000370065	0,000567041	0,000809873	0,001095012
η(100)	2,20306E-05	3,70065E-05	5,67041E-05	8,09873E-05	0,000109501
η(1000)	2,20306E-06	3,70065E-06	5,67041E-06	8,09873E-06	1,09501E-05
η(10000)	2,20306E-07	3,70065E-07	5,67041E-07	8,09873E-07	1,09501E-06

parametro di vista	r=110nm	r=120nm	r=130nm	r=140nm	r=150nm
η(10)	0,001418082	0,001775128	0,002163503	0,002582311	0,00303242
η(100)	0,000141808	0,000177513	0,00021635	0,000258231	0,000303242
η(1000)	1,41808E-05	1,77513E-05	2,1635E-05	2,58231E-05	3,03242E-05
η(10000)	1,41808E-06	1,77513E-06	2,1635E-06	2,58231E-06	3,03242E-06

Table of linear attenuation coefficients expressed in μm^{-1}, as a function of the density of the particle number and the radius.

Optical losses as a function of radius and densities

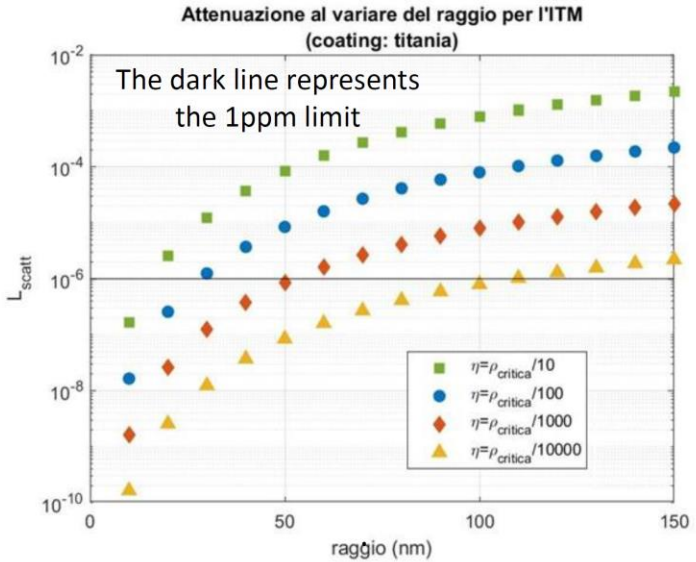

.

The current Advanced Virgo scattering losses are estimated to be at 10 ppm per mirror (J. Degallaix)

Titania (TiO_2) ETM

parametro di vista	r=10nm	r=20nm	r=30nm	r=40nm	r=50nm
η(10)	7,81237E-08	1,2178E-06	5,90649E-06	1,76026E-05	3,99341E-05
η(100)	7,81237E-09	1,2178E-07	5,90649E-07	1,76026E-06	3,99341E-06
η(1000)	7,81237E-10	1,2178E-08	5,90649E-08	1,76026E-07	3,99341E-07
η(10000)	7,81237E-11	1,2178E-09	5,90649E-09	1,76026E-08	3,99341E-08

parametro di vista	r=60nm	r=70nm	r=80nm	r=90nm	r=100nm
η(10)	7,59423E-05	0,000127566	0,000195467	0,000279174	0,000377465
η(100)	7,59423E-06	1,27566E-05	1,95467E-05	2,79174E-05	3,77465E-05
η(1000)	7,59423E-07	1,27566E-06	1,95467E-06	2,79174E-06	3,77465E-06
η(10000)	7,59423E-08	1,27566E-07	1,95467E-07	2,79174E-07	3,77465E-07

parametro di vista	r=110nm	r=120nm	r=130nm	r=140nm	r=150nm
η(10)	0,000488832	0,00061191	0,000745788	0,000890157	0,001045315
η(100)	4,88832E-05	6,1191E-05	7,45788E-05	8,90157E-05	0,000104532
η(1000)	4,88832E-06	6,1191E-06	7,45788E-06	8,90157E-06	1,04532E-05
η(10000)	4,88832E-07	6,1191E-07	7,45788E-07	8,90157E-07	1,04532E-06

Table of linear attenuation coefficients expressed in μm^{-1}, as a function of the density of the particle number and the radius.

Optical losses as a function of radius and densities

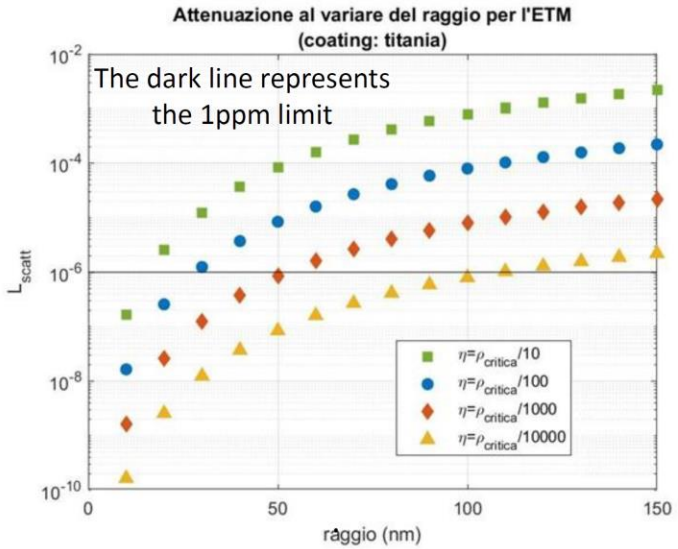

The current Advanced Virgo scattering losses are estimated to be at 10 ppm per mirror (J. Degallaix)

Conclusions (2)

- The graphs show, as a first approximation, the optical losses, defining for which values of the densities and radii, are below 1 ppm, (i.e. below 1/10 of the limits required for Advanced Virgo).

- To further validate the analysis, the data from these simulations can be compared with experimental measurements; in particular with calorimetry measurements (density of crystallites), as well as with scattering measurements.

- if the simulations respect the experimental data they can be used as a guide to see how big the densities and radii can be to avoid optical losses.

Future Simulations

Future simulations that deepen what has been found so far could be developed for non-spherical particles. A method for calculating the scattering cross section of such objects is described in:

Scattering and Absorption of Light by Nonspherical Dielectric Grains
-Purcell, Edward M.; Pennypacker, Carlton R. *Astrophysical Journal*, Vol. 186, pp. 705-714

and it is valid for particles of a smaller size or comparable with the incident wavelength, a criterion which, as we have shown, is respected by our nanocrystals. For an even more accurate treatment, the phenomenon of multiple scattering from nano-diffusers could be simulated using an extension of the Mie theory, for more spheres, present in:

The Extension of Mie Theory to Multiple Spheres
D. Mackowski, *Springer Series in Optical Sciences*, vol 169, https://doi.org/10.1007/978-3-642-28738-1_8